Herance, JR.; García Gómez, H.; Guitierrez Carcedo, P.; Navalón Oltra, S.; Pineda-Lucena, A.; Palomino-Schätzlein, M. (2019). A translational approach to assess the metabolomic impact of stabilized gold nanoparticles by NMR spectroscopy. The Analyst. 144(4):1265-1274. https://doi.org/10.1039/c8an01827h

A translational approach to assess the metabolomic impact of stabilized gold nanoparticles by NMR spectroscopy

José Raul Herance,*[a] Hermenegildo García[b], Patricia Gutiérrez-Carcedo[a], Sergio Navalón[c], Antonio Pineda-Lucena[d,e] and Martina Palomino-Schätzlein*[e]
a Vall d'Hebron Research Institute, CIBBIM-Nanomedicine, CIBERbbn, Barcelona, Spain
b Instituto Universitario de Tecnología Química CSIC-UPV, Valencia, Spain.
c Escuela Técnica Superior de Ingeniería Industrial, Universitat Politècnica de València, Valencia, Spain.
d Instituto de Investigación Sanitaria La Fe, Hospital Universitario i Politécnico La Fe, Valencia, Spain.
e Centro de Investigación Príncipe Felipe, Valencia, Spain.

*Corresponding authors:
E-mail: mpalomino@cipf.es
E-mail: raul.herance@vhir.org

Abstract

Gold nanoparticles have a high potential in the biomedical area, with a special emphasis in disease diagnosis and treatment. The application of these nanoparticles requires the presence of stabilizers to avoid their agglomeration. Nowadays, there is a lack of reliable methods for characterising the effect of stabilised nanoparticles on biological systems. To this end, in this study, we apply an experimental approach based on nuclear magnetic resonance spectroscopy to study the effect of gold nanoparticles, stabilised with cerium oxide or chitosan on a human cancer cell model. The results showed that both systems have a significant effect, even at non-toxic levels, on the cellular antioxidant system. However, although particles functionalised with chitosan exerted a strong effect on the aerobic respiration, nanoparticles stabilised with cerium oxide had a higher impact on the mechanisms associated with anaerobic energy production. Therefore, even though that both systems contained similar gold nanoparticles, the presence of different stabilizers strongly influenced their mode of action and potential applications in biomedicine.

Introduction

The application of nanomedicine, that is, the utilisation of nanotechnology in medical research and clinical usage, has grown exponentially in the last few years, improving traditional therapeutic and diagnostic procedures.[1] Gold nanoparticles (AuNPs) have unique chemical properties including stability, inertness and tunability of size, shape, or surface chemistry[2], thus facilitating their use as nanomedicines with a wide range of applications. Currently, they are used as agents for cell imaging, targeted drug delivery, diagnosis and therapy[3], and they have become an important tool in different medical specialities, most notably in cancer research.[4–8] *In vivo* studies have shown that AuNPs can circulate in blood for a prolonged time period and accumulate in the tumor, due to the enhanced permeability and retention (EPR) effect.[9] Furthermore, the physical properties and tailored surface functionalisation of AuNPs make them excellent candidates as theranostic agents, as well as radiosensitisers to locally increase the damaging effect of both photon and ion radiation.[6,10]

AuNPs need to be stabilised by the use of agents, known as stabilisers, which avoid the agglomeration of NPs. To this end, several stabilisers have been introduced, using different experimental approaches, such as covering the NPs with polymers or charged organic chains, supporting them on metal oxides or functionalising them.[11] The stabiliser can change the properties of AuNPs influencing both their toxicity and biomedical applications. For example, gold-supported ceria NPs ($AuCeO_2$) are an excellent system for modulating the oxidation state of AuNPs.[12] Thus, it has been shown that the presence of Au on $AuCeO_2$ increases the ability of

ceria to neutralise reactive oxidant species (ROS) under oxidative stress conditions.[13] However, although biocompatibility assays suggest that $AuCeO_2$ NPs do not induce lethal damage in the cell, further studies will be required to assess their impact in the potential transformation of cytosolic biomolecules or their effects on metabolic pathways. Furthermore, functionalisation of AuNPs with chitosan (AuChi), a biopolymer obtained by deacetylation of chitin from the exoskeleton of crustacea and approved by the regulatory agencies for medical uses[14], has been proposed to modulate the biocompatibility and the antioxidant behaviour of Au and to increase their bactericidal effect.[2] AuChi has been proposed for chemo-radiotherapeutic purposes[15], as well as a suitable system for releasing drugs[16], genes[17] and as diagnostic agents[18], among others.

However, the development of these NPs, and others, is still at a very early stage. In this context, and despite the increasing number of reports describing the application of NPs in medicine, there is a lack of suitable methods guaranteeing the safe application of these novel nanomedicines. Therefore, new approaches are required to characterise in detail the effects of nanomaterials on biological systems.[19]

Omics approaches provide highthroughput methods in medical diagnostics for the analysis of disease states or predictive toxicology.[3] In particular, metabolomics, relying on the analysis of the complete set of low molecular weight compounds in a biological sample, has the advantage of revealing the phenotype of a cell/tissue at a particular time under specific physiological or therapeutic conditions. Thus, metabolomics represents an ideal strategy for investigating the interaction between NPs and biological systems at different molecular levels.[20] Nuclear magnetic resonance (NMR) spectroscopy, a robust, reproducible and fast analytical method for identifying and quantifying metabolites in cells [21], is a suitable tool for metabolomics profiling. In this context, a series of metabolomics studies, focused on different model systems, have been recently published describing alterations in different metabolic pathways due to the presence of specific NPs.[19,20,22] In particular, several metabolomics studies, based on the effects of AuNPs, have provided insights into their mechanism of action[3,23] revealing that they can bind to intracellular metabolites,[24] influence different metabolic processes (energy and choline metabolism, HBP pathway, oxidative stress[25]), lead to cell apoptosis[26] and affect cancer cells differently from healthy cells[27].

Therefore, metabolomics could provide a suitable approach for characterising the effect of the stabilizer on the biological properties of AuNPs. In particular, the aim of this work was to evaluate the impact of $AuCeO_2$ and AuChi, on HeLa cells by NMR spectroscopy. These stabilizers were selected based on their promising applications in biomedicine, as they both are antioxidants and biocompatible. However, their different geometries (AuChi: coating, $AuCeO_2$:

supported) and charges could potentially influence their mechanisms of action. We wanted to assess whether metabolomics could characterise the biochemical impact of both NPs to a better extent that the routine tests that are traditionally performed at the preclinical stage. Our analysis of the metabolomic and protein profile revealed a significant effect on cell metabolism, even at non-toxic levels, of cell treated with AuNPs.

Methods

Chemicals and materials. Solvents and reagents were purchased from: Sigma-Aldrich (PBS, fetal bovine serum, penicillin, streptomycin, amphotericin B, L-glutamine, chitosan, $HAuCl_4$, sodium citrate, $AgNO_3$, sodium phosphate dibasic dihydrate, CeO_2), Scharlab (methanol, chloroform, acetone, sodium hydroxide), Gibco (DMEM), and Eurisotop (deuterated water, deuterated chloroform, deuterated trimethylsilyl propanoic acid, trimethylsilane, 5 mm NMR tubes). Materials were purchased from Scharlab, Life Technologies, and Falcon BD. Gases were supplied by Air-Liquide.

Synthesis and characterisation of gold-chitosan nanoparticles (AuChi)

AuChi nanoparticles were synthesised as previously reported[28] with minor modifications. Briefly, 200 mg of low molecular weight chitosan were added to 100 mL of milliQ water with 1% of acetic acid. After heating this solution at 90 ºC, 1.3 mL of a 9.6 mM $HAuCl_4$ aqueous solution were slowly added, and the mixture was stirred for 5 min. Then, 250 µL 0.1 M sodium citrate solution was poured into the mixture and stirred for an additional 5 min. Afterwards, the solution was cooled and filtered through a 0.22 µm filter before being characterised by dynamic light scattering (DLS) (Zetasizer Nano ZS, Malvern Instrument, UK), high resolution transmission electron microscopy (HR-TEM) (Philips CM300FEG 100 kV) and inductively coupled plasma (ICP) (Varian 715-ES ICP-Plasma). The stability of AuChi NPs in PBS was evaluated as previously described[29] following the stability of the NPs (20 µg/mL in DMEM or PBS) by DLS at different time points (24, 48, and 72 h).

Synthesis and characterization of gold-ceria nanoparticles ($AuCeO_2$)

$AuCeO_2$ was prepared as previously reported by our group.[13] Briefly, 0.2 M NaOH was added to a solution containing 200 mg of $HAuCl_4$ in 40 mL of milliQ water until reaching pH=10 with vigorous stirring. Then, 1.0 g CeO_2 dissolved in 13 mL of milliQ water was added slowly, adjusting the pH to 10 with 0.2 M NaOH. Subsequently, the mixture was stirred vigorously overnight at room temperature. Then, the solid was washed with milliQ water and dried at 50°C

overnight. Afterwards, the sample was heated from room temperature to 300ºC at 8°C/min for 4.5 h in a H_2 atmosphere. Following this step, the furnace was shut down until reaching room temperature. Then, nanoparticles were dissolved in PBS, filtered through a 0.22 µm filter, and characterised by HR-TEM (Philips CM300FEG 100 kV), DLS (Zetasizer Nano ZS, Malvern Instrument, UK), and ICP (Varian 715-ES ICP-Plasma). The stability of the $AuCeo_2$ in PBS was assessed as previously reported[29].

Cell culture

HeLa cells (ATCC CCL-2) were cultured (37ºC, 5 % CO_2 atmosphere) using P150 plates until reaching 75% confluence, starting with 25000 cells/cm^2 in DMEM medium with high glucose concentration (4.5 mg/mL) and supplemented with 10% FBS, penicillin (50 units/mL), and streptomycin (50 µg/mL). After 24 h of incubation, cells were treated with NPs at 20 µg/ml for 24, 48 and 72h in DMEM medium. Then plates were put on ice, the medium was discarded, and cells were washed with 10 ml of ice-cold PBS. Then, an additional 10 ml of PBS were added and cells were scraped off. The cell suspension was centrifuged at 300 g and the supernatant discarded. The resultant pellet was washed once with PBS and 0.5 ml of ice-cold methanol was added to the final pellet to quench metabolism. Samples were stored at -80°C until sample preparation and measurement. Nine independent replicates were performed at 3 different culture days.

For sample preparation, frozen samples were placed on ice and allowed to thaw for 5 min. Then, 500 µL of chloroform at 4 °C were added, and 10 min later the samples were homogenized with a vortex and resuspended. To induce an uniform cell breakage, samples were placed in liquid nitrogen for 2 min and then allowed to thaw on ice for 4 min. This step was repeated twice. Afterwards, 780 µL of deionized water and 780 µL of chloroform at 4 °C were added and the sample vortexed. Then, the samples were centrifuged at 10000 g for 15 min at 4 °C to allow phase separation into an aqueous and an organic phase. The aqueous phase was separated and lyophilized overnight to remove water and methanol.

For NMR measurements, 550 µl of phosphate buffer (100 mM Na_2HPO_4 pH 7.4, in 100% D_2O) containing 0.1 mM 3-(trimethylsilyl)propionic-2,2,3,3-d4 acid sodium salt (TSP), as internal standard, were added to the lyophilized aqueous phase. Samples were vortexed and the supernatant was transferred into a 5 mm NMR tube.

NMR spectroscopy

NMR spectra were recorded at 27°C on a Bruker AVII-600 using a 5 mm TCI cryoprobe and processed using Topspin 3.5 software (Bruker GmbH, Karlsruhe, Germany). ^{1}H-NMR spectra

with water presaturation and a 10 ms noesy mixing time were acquired for cell extracts with 128 free induction decays (FIDs). 64k data points were digitalised over a spectral width of 30 ppm. A 4 s relaxation delay was included between FIDs. The FID values were multiplied by an exponential function with a 0.5 Hz line-broadening factor. Total Correlation Spectroscopy (TOCSY) and multiplicity Heteronuclear Single Quantum Correlation (HSQC) were performed for representative samples to facilitate chemical shift assignment. For each of these experiments, 256 t1 increments were used and 16-64 transients were collected. The relaxation delays were set to 1.5 s and the experiments were acquired in the phase-sensitive mode. TOCSY spectra were recorded using a standard MLEV-17 pulse sequence with mixing times (spin-lock) of 65 ms. NMR spectra were Fourier transformed and processed with a line broadening factor of 0.5. Phase and base line were corrected automatically. Assignment of the chemical shifts was performed using HMBD in combination with the BMRB database.[30,31] Identified metabolites were integrated in MestreNova 10 with GSD deconvolution.

MTT assay

The MTT [3-(4,5-dimethylthiazol-2-yl)-2,5-diphenyltetrazolium bromide] cell viability assay[32] was carried out using the Cell Proliferation Kit from Roche Sigma Aldrich (Cat. No. 11465 007 001). Stock solution of NPs (20 mg/mL of AuChi, 5.5 mg/ml of $AuCeO_2$) in milliQ water were prepared with sonication. These stock solutions were diluted in DMEM to achieve 10, 20, 100, and 1000 µg/mL solutions. HeLa cells were harvested at their logarithmic phase and seeded at concentrations of 35000 cells per well in 96-well microliter plates with a final volume of 200 µl in DMEM medium. After incubation of 24 h at 37 °C and 5% CO_2, medium was replaced for a new medium with NPs. Cells were incubated in the presence of NPs for 24, 48 and 72 h, and then replaced by fresh medium without NPs. Then, 100 µl of medium was taken from each well, and 10 µl of MTT reagent (final concentration 0.5 mg/ml) was added. After 4 hours, 100 µl of solubilisation solution was added, and cells were left overnight. Finally, the absorbance was measured with a spectrophotometer (Synergy Mx plate reader, BioTek Instruments, Winooski, VT) at 690 and 550 nm. Results are reported as the mean of triplicates of three independent experiments.

Cellular uptake and internalisation of conjugate by confocal microscopy

Experiments were performed as described in previous works.[33,34] Briefly, HeLa cells were seeded at $8x10^5$ per dish in Nunc™ Glass culture dishes. After 24 h, NPs (AuChi and AuCeO2) were added at 20 µg/mL and incubated for 24h. Nuclei (Hoechst 33342 dye, 1:20000 dilution,

blue) (Life Technologies, Madrid, Spain) and cell membranes (CellMaskTM, 1:10000 dilution, green) (Life Technologies, Madrid, Spain) were stained following manufacturer's protocol.[1,2] Fluorescence images were obtained *in vivo* with an Olympus (FV1000-spectral) confocal microscope. Samples were maintained at 37°C under 5% CO2 atmosphere during imaging and were illuminated simultaneously with laser light at 405 nm (exciting Hoechst, blue), and 488 nm (exciting CellMask, green) recording the emission from 415 to 603 nm in separate channels. The reflection signal of NPs was split by using a dichroic mirror (20/40) after irradiating at 633 nm. Z-stack study across the depth of the cells was recorded with an interslice distance of 400nm. Fiji ImageJ program was used to analyse the images.

Western Blot

Total protein extracts from cell pools were obtained after lysis with an extraction buffer (20 mM HEPES pH 7.5, 400 mM NaCl, 20 % Glycerol, 0.1 mM EDTA, 10 µM Na_2MoO4, 0.5 % NP-40) containing protease inhibitors (10 mM NaF, 1 mM $NaVO_3$, 10 mM PNP, 10 mM β-glycerolphosphate) and 1 mM dithiothreitol after incubating for 15 min on ice and centrifuged at 4 °C for 15 min. Protein was quantified using the BCA protein assay kit (Thermo Scientific, Rockford, USA). 25 µg of protein were resolved by sodium dodecyl sulphate polyacrilamide gel electrophoresis (SDS-PAGE) and then transferred to nitrocellulose membranes and incubated with antibodies (Thermo Scientific, Rockford, USA) at different dilutions: Actin (rabbit 1:2000), NrF1 (rabbit 1:1500), NrF2 (rabbit 1:1000), SOD1 (rabbit 1:1000), CAT (rabbit 1:8000), GR (rabbit 1:8000), GPX1 (rabbit 1:1500), LC3 (rabbit 1:500), and LDH-A (mouse 1:800). HRP-goat anti-mouse (Thermo Scientific, Rockford, USA) and peroxidase goat anti-rabbit (Vector laboratories, Peterborough, UK) were used as secondary antibodies. The protein signal was detected by chemiluminescence, after incubating membranes with ECL plus reagent (GE healthcare, Uppsala, Sweden) or Supersignal West Femto (Thermo Scientific, Rockford, USA), and was visualised in a Fusion FX5 acquisition system (Vilbert Lourmat, Marne La Vallée, France).

Data analysis

NMR data table were normalized to total intensity, mean centered and scaled to unit variance to perform multivariate data analysis (SIMCAP 14, Umetrics, Sweden). Principal components analysis (PCA) was used to examine clustering trends between samples, correlations between metabolite concentrations, and the presence of strong outliers. Analysis of metabolic pathways was performed using Metaboanalyst.[35]

For western blot analysis, signals were analysed and quantified by densitometry using Bio1D software (Vilbert Lourmat, Marne La Vallée, France). Protein bands were normalised to the expression of actin in the same sample.

For MTT, results were obtained by subtracting the absorbance at 690 nm from the 550 nm following the kit instructions. Data analysis was performed with SPSS 17.0 and expressed as relative to control ± SEM, with the negative control (untreated cells) being considered 1.

Univariate analysis was performed with R.

Results

Synthesis of nanomaterials

Gold nanoparticles stabilised on cerium oxide ($AuCeO_2$) or functionalised with chitosan (AuChi) were synthetized as previously reported.[13, 28] The physical characterisation of both NPs revealed mean sizes, determined by HR-TEM, of 5.9 nm ($AuCeO_2$) and 5.7 nm (AuChi) (Supplementary Figures 1 and 2). Moreover, hydrodynamic sizes, measured by DLS, of 112.0 nm ($AuCeO_2$) and 104.3 nm (AuChi) (Supplementary Figures 3 and 4), and a gold content, determined by ICP, of 0.8 % ($AuCeO_2$) and 1.2 % (AuChi) was obtained for both NPs. Finally, the measurement of net zeta potentials resulted in + 17 mV (AuChi) and -19 mV ($AuCeO_2$), thus indicating that, even though the two stabilisers resulted in gold NPs of similar size, they provided opposite net charges. Stability of both NPs was confirmed by measuring the hydrodynamic size (DLS) of both nanoparticles during 72 h in PBS (Supplementary Figures 5 and 6).

Toxicity and internalisation of nanomaterials

The toxic effect of the nanomaterials was evaluated by the MTT cell viability assay[32] in HeLa cells lines in the presence or absence of NPs. These analyses were performed, at four different concentrations (10, 20, 100 and 1000 µg/ml) and time points (24, 48 and 72 h), to assess the effect on cell viability and proliferation. While a significant growth decrease could be detected at 100 and 1000 µg/ml, this was not the case at lower concentrations (10 and 20 µg/ml) (Figure 1). However, it has been reported[36] that the MTT assay could provide misleading results on cell viability in the presence of NPs, as they can interfere at different levels in this assay. Therefore, it could be interesting to complement these studies with other experimental approaches to obtain an accurate description of the effect of NPs on biological systems. As neither 10 µg/ml nor 20 µg/ml did induce any change of cell viability and proliferation, 20 µg/ml was chosen as cell concentration to see more pronounced changes of cell metabolism.

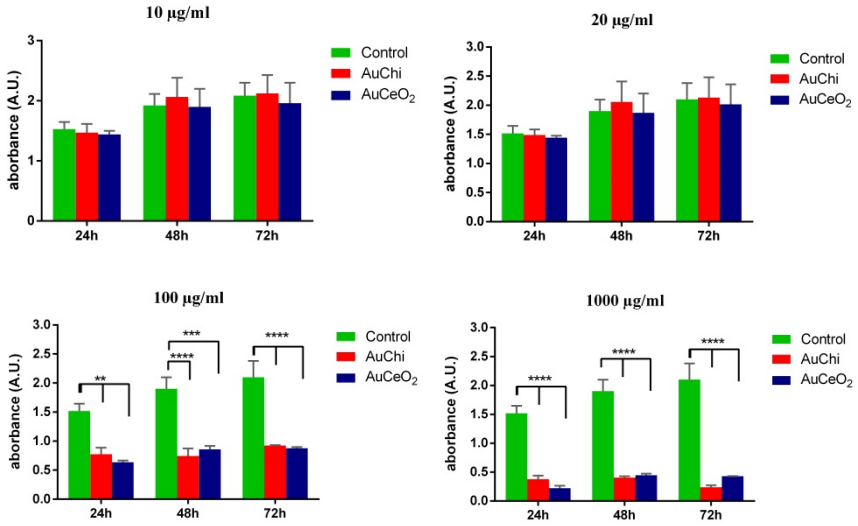

Figure 1. MTT assay of HeLa cells treated with AuChi and $AuCeO_2$ NPs obtained at different concentrations (10, 20, 100 and 1000 µg/ml) and time points (24, 48 and 72 hours). Statistical significance: ** ($p < 0.01$), *** ($p < 0.001$) **** ($p<0.0001$)

The internalisation of the NPs into the cells was followed by confocal microscopy. The resulting images (Supplementary Figure 7) confirmed that both AuChi and $AuCeO_2$ NPs were internalised into the cells under the specified experimental conditions, as it has been observed in previous studies.[37–39]

Metabolomic profiling

^{1}H-NMR spectra were obtained from aqueous extracts of HeLa cells cultured during 24, 48 and 72 hours in the presence of AuChi and $AuCeO_2$ nanomaterials (dose 20 µg/ml) and without treatment (CT). The analysis of the spectra revealed that the most significant differences between the metabolic profiles were detected at 48 and 72 h Representative spectra at these time points with the different treatments are represented in Figure 2.

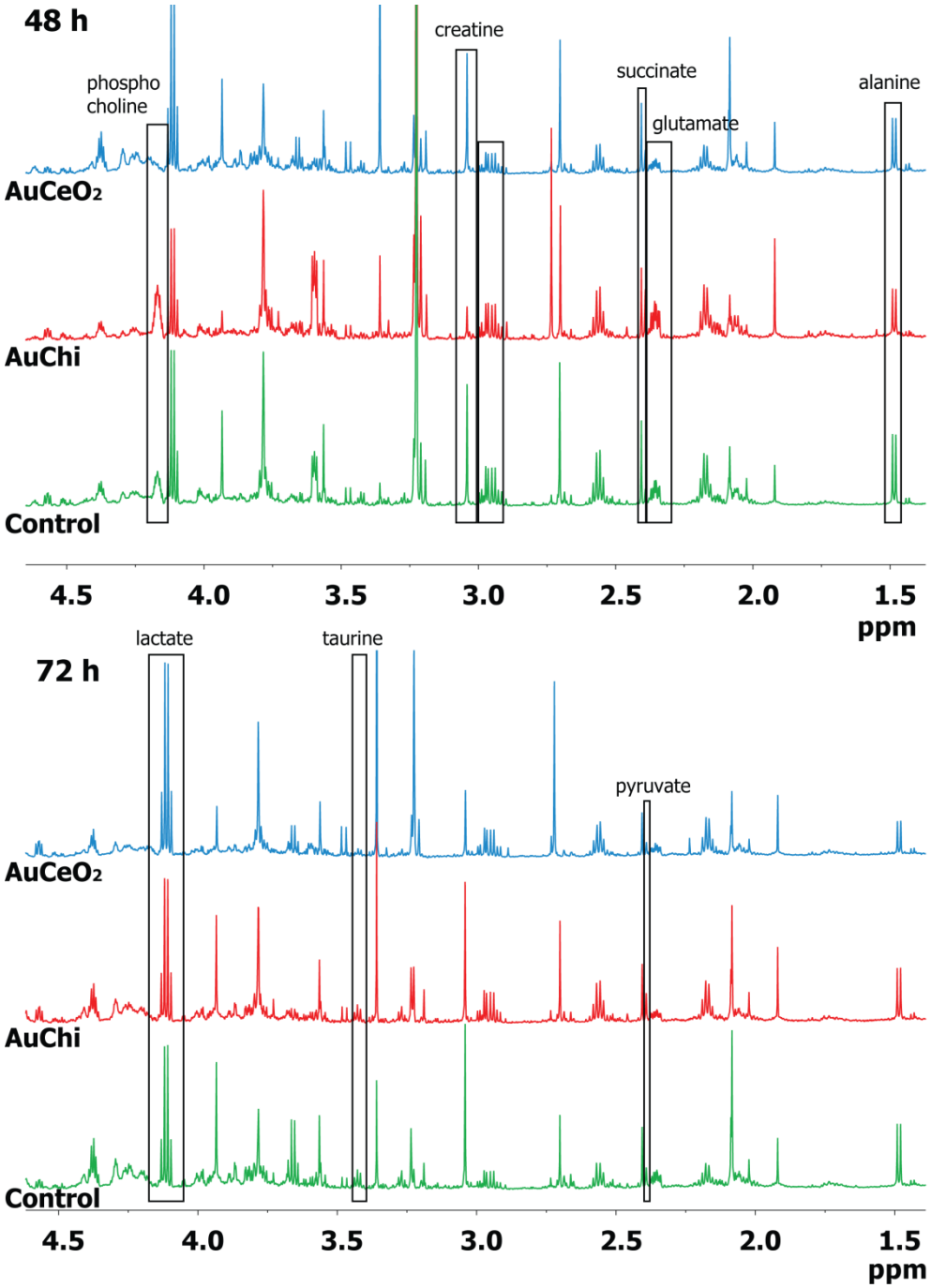

Figure 2. Representative ^{1}H-NMR spectra of aqueous cells extracts of HeLa cells, obtained in the presence (Control) or absence of $AuCeO_2$ and AuChi NPs (20 µg/ml) at two different time points (48 and 72 h), illustrating some of the most significant metabolic alterations under these experimental conditions. Spectra were acquired at 600 MHz, 27 °C with an inverse cold probe and 128 free induction decays.

A principal component analysis (PCA), based on the NMR data, was performed to get an overview of the metabolic changes induced by both NPs, and the corresponding score plots obtained at the different time points (24, 48 and 72 h) are shown in Figure 3.

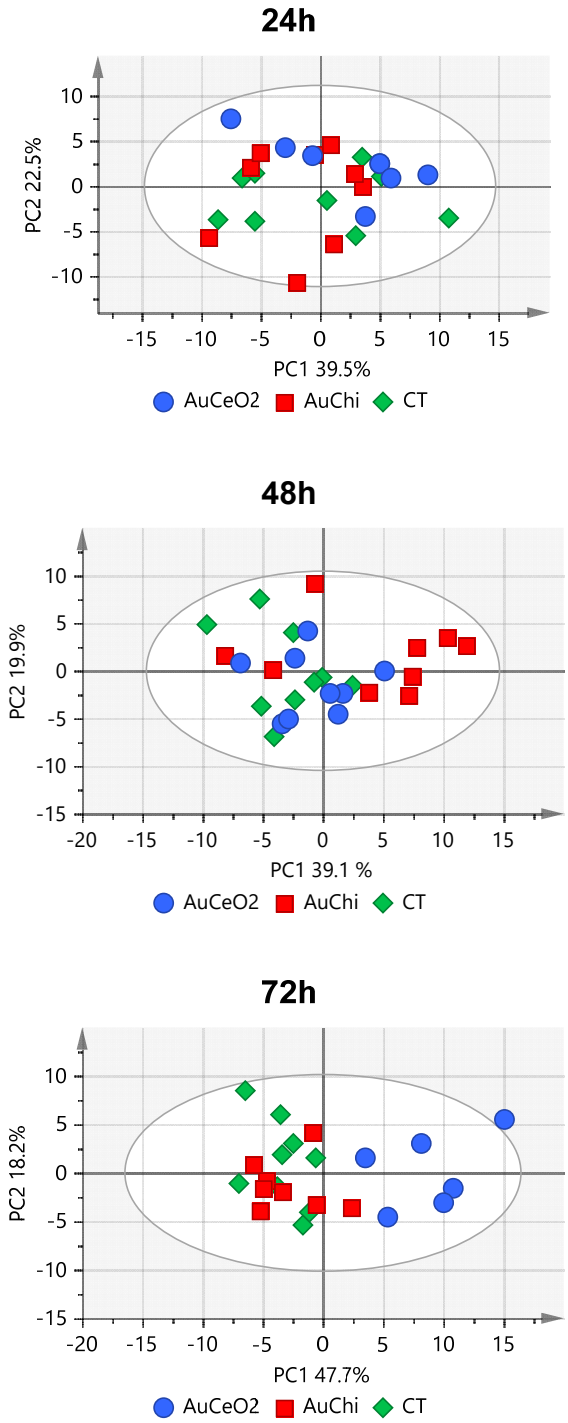

Figure 3. PCA score plots of the first two components. of metabolic profiles of HeLa cell extracts from untreated (CT) cells and cells treated with AuChi and $AuCeO_2$ at 24, 48 and 72 hours. Model at 24h: R2X (cum) = 0.773, Q2 (cum) = 0.513, 4 components. Model at 48h: R2X (cum) = 0.79, Q2 (cum) = 0.541, 4 components. Model at 72h: R2X (cum) = 0.756, Q2 (cum) = 0.572, 3 components. Data were scaled to unit variance. The units on the axes denote the raw component scores and are not directly interpretable. The total variance captured by each principal component is indicated on the axes.

The analysis of the PCA score plots confirmed the absence of clear metabolic differences at 24 h between untreated or treated HeLa cells (Figure 3, top panel). However, AuChi NPs induced significant metabolic differences at 48 h, as observed by the clustering of samples on the right side (Figure 3, middle panel) compared to the left side of the score plot ($AuCeO_2$ and untreated cells). Finally, the score plots revealed that $AuCeO_2$ NPs induced metabolic alterations after longer time periods (Figure 3, bottom panel). Taken together, these results clearly indicated relevant differences in the mode-of-action and dynamics of both NPs.

To get a deeper insight into the metabolic alterations associated with the treatment with both NPs, relative concentrations of selected metabolites were calculated under the different experimental conditions (Supplementary Tables 1-2, Figure 4). The results clearly showed that, even though both NPs did not induce a significant decrease in general growth, they affected several metabolic pathways.

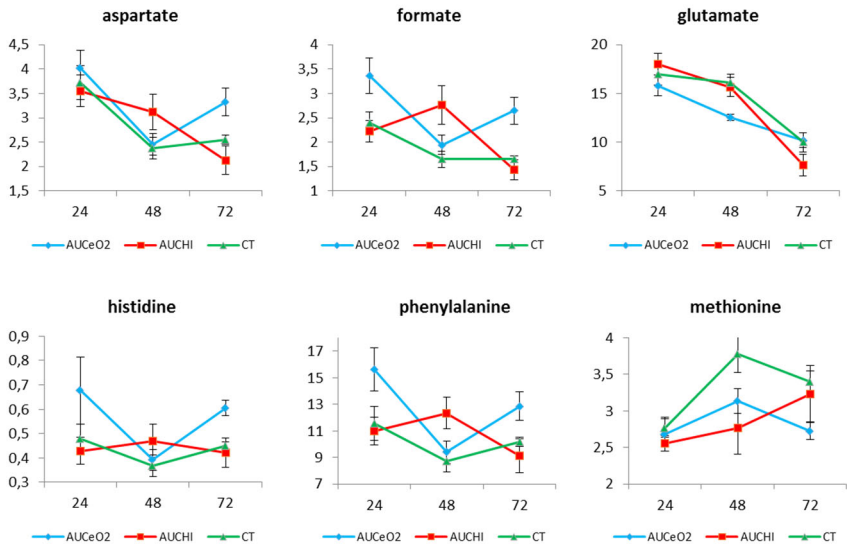

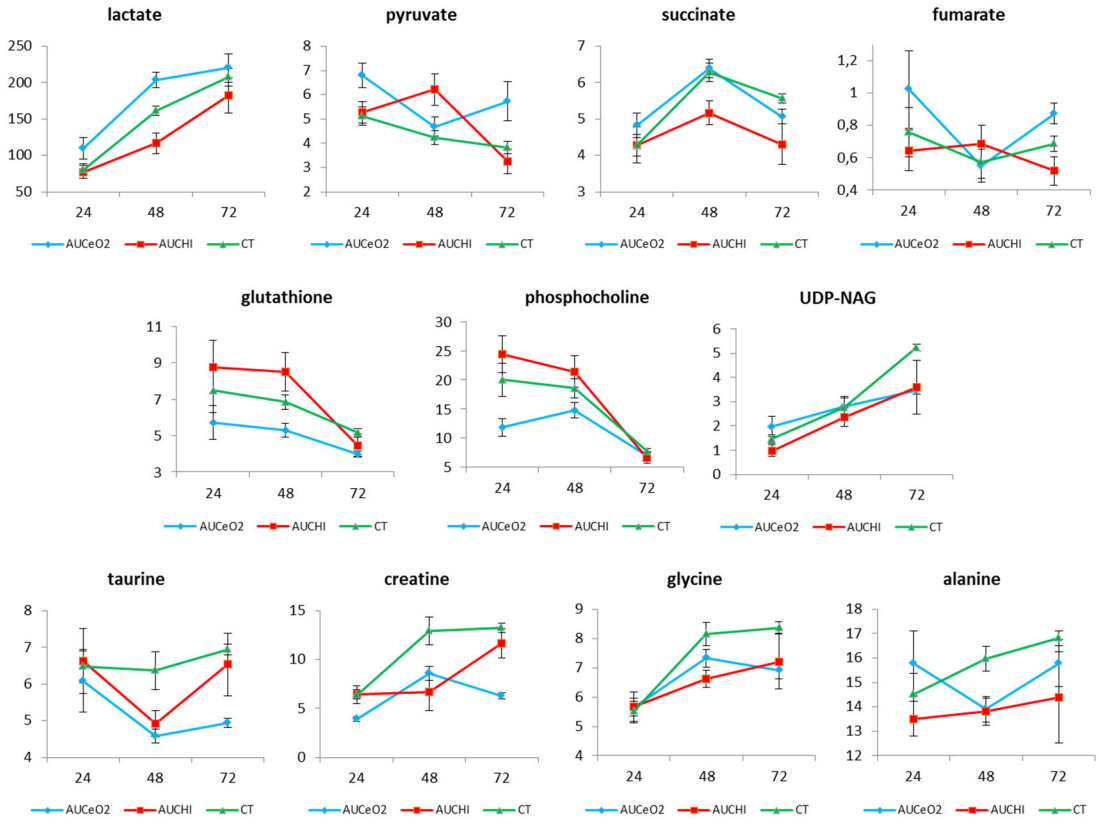

Figure 4. Normalized concentration values of selected metabolites after 24, 48 and 72 h treatment in the absence (CT) or presence of $AuCeO_2$ or AuChi NPs. Concentrations are expressed as mean±SEM.

Interestingly, although the size of both NPs was quite similar, the dynamics of the metabolic alterations were different, as already suggested by PCA analysis. Thus, significant increases (aspartate, formate, phenylalanine, histidine, and glutamate) or decreases (methionine) in the levels of several metabolites were observed at 48 h for AuChi NPs, but only at 72 h for $AuCeO_2$ NPs. In particular, pyruvate, a key metabolite resulting from glycolisis, was clearly increased by AuChi NPs at 48h, but increased by $AuCeO_2$ at 72 h.

Moreover, some metabolic changes exhibited opposite signs when HeLa cells were treated with both NPs. Thus, lactate levels, a metabolite generated from the anaerobic metabolism of pyruvate, were decreased after treatment with AuChi NPs, but increased by $AuCeO_2$ NPs. Furthermore, metabolites from citric acid cycle were also differently altered by AuChi and $AuCeO_2$ NPs. While succinate followed a very similar pattern for untreated and $AuCeO_2$ NPs (a decrease from 24 to 48 h, and an increase from 48 to 72h), this increase was less pronounced for AuChi treated cells. On the other hand, fumarate levels decreased from 24 to 48 h and increased from 48 to 72 h for untreated and $AuCeO_2$ cells, which was not the case for AuChi cells.

A different behaviour was also observed glutathione and phosphocholine (associated with the antioxidant protection of the cells). The results showed that the levels of these metabolites were significantly higher after 48 h for AuChi NPs treated HeLa cells, but lower for those treated with $AuCeO_2$ NPs.

Finally, some metabolic alterations were similar for both NPs (e.g., alanine, taurine, creatine and glycine). The levels of all of them were decreased by both NPs after 48 h of treatment, while UDP-NAG was decreased only after 72 h. However, the magnitude of the changes associated with the levels of taurine and creatine was more important in the presence of $AuCeO_2$ NPs at 72 h.

Protein expression.

To better assess the impact of the treatment with both NPs, the levels of several key proteins (i.e., lactate dehydrogenase (LDH), glutathione peroxidase 1 (GPX1), nuclear respiratory factor 2 (NRF2), nuclear respiratory factor 1 (NRF1), glutathione reductase (GR), catalase (CAT)) were quantified by western blot analysis in untreated, and $AuCeO_2$ and AuChi NPs treated cells, at different time points (24, 48 and 72 h) (Figure 5). Due to the critical role of these proteins in cell function (apoptosis, mitochondrial function, endogenous antioxidant system), the measurement of their levels could provide very relevant information regarding the toxicity and the impact on the antioxidant capacity of the cells in the presence of both NPs. In general, the observed changes were moderate, with the exception of those associated with GPX1 and NRF1, two proteins involved in the antioxidant capacity of the cells and in mitochondrial function, respectively. The levels of GPX1 were significantly decreased in the presence of both NPs, probably reflecting the antioxidant properties of these NPs, as it was previously reported[40]. On the other hand, the effect on the levels of NRF1 was different for the two NPs. A significant decrease was observed in the presence of AuChi NPs at all times; however, NRF1 levels decreased at 24 and 72 h in the presence of $AuCeO_2$, but increased at 48 h. Interestingly, a slight increase in the levels of NRF2 was also observed at 48 h in the presence of $AuCeO_2$, perhaps indicating a regulation of antioxidant enzymes that could be associated with the changes observed for NRF1. Finally, LDH levels experienced a decrease in the presence of AuChi NPs and a tendency to increase when cells were treated with $AuCeO_2$ NPs, thus suggesting less toxicity associated with the presence of AuChi compared to $AuCeO_2$ NPs. No significant changes were observed in the levels of CAT and GR.

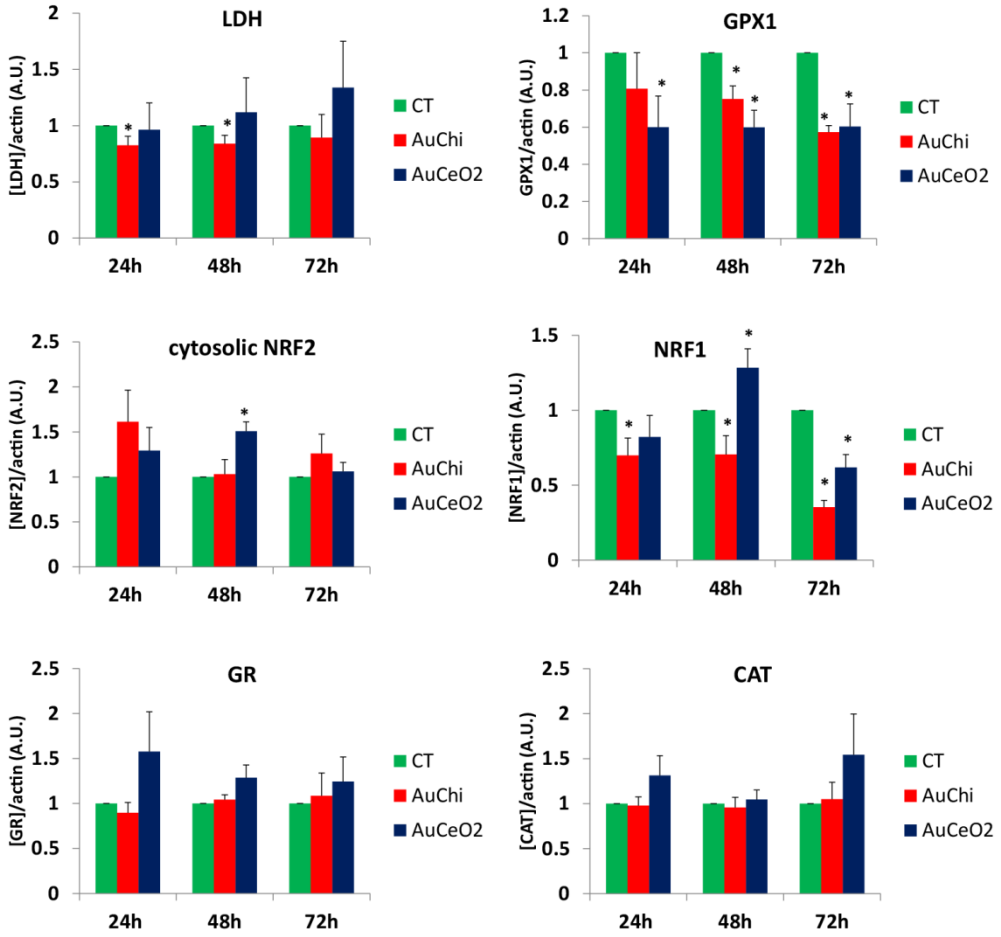

Figure 5. Protein expression levels, normalized to those of control cells, for LDH, GPX1, cytosolic NRF2, NRF1, GR and CAT. Statistical significance: * ($p<0.05$)

Discussion

The results of this study show that both stabilised AuNPs had an impact on cell metabolism, even at non-toxic concentrations as detected by the MTT assay; this finding being in agreement with previous metabolomics studies based on the utilisation of NPs[41]. Nevertheless, as shown in Supplementary Figures 8-10, both NPs caused important metabolic alterations, although the expression of key proteins underwent less severe changes (Figure 5). Interestingly, and despite the fact that both NPs had a similar size, the presence of different stabilisers induced metabolic changes at different time points; thus, the maximum biochemical effect of AuChi NPs was achieved at 48 h, but $AuCeO_2$ NPs required a longer period of time, 72 h. The existence of these temporal differences at the biochemical level confirms the need to perform longitudinal studies when comparing the metabolomic impact and the pharmacodynamics of different NPs. A potential explanation for these changes could be partially ascribed to the different charge of both NPs. Thus, it is possible that the positively charged AuChi

NPs could be more easily internalised based on their stronger interaction with the negatively charged cell membrane, while this process would take longer for the negatively charged $AuCeO_2$ NPs. This result would be in agreement with previous reports describing different effects for negatively and positively charged NPs[42], in particular, for 16HBE cells treated with Au nanoroids.[25]

A number of specific metabolic changes were observed in the presence of both NPs, including alterations in the levels of taurine, glycine, serine and threonine at 48 h (Supplementary Figure 8). Taurine and glycine have been associated with the oxidative system of the cells. In this context, taurine is known to protect against oxidative stress and inflammation by scavenging reactive oxygen species[43], and decreased levels of this metabolite have been previously reported upon treatment with NPs able to scavange free radicals and oxidants, such as ZnO_2[44] and silica particles.[45] On the other hand, glycine is a precursor of glutathione, one of the main endogenous antioxidant systems of the cell, and its decrease has been already described in cells treated with NPs that can scavenge free radicals, such as zinc, silica, titanium and capped gold NPs[24,44–46]. In agreement with this finding, it was observed that GPX1 protein levels decreased in the presence of both NPs. However, GR protein levels had a tendency to increase after treatment with $AuCeO_2$ NPs at 48 h, but not in the presence of AuChi NPs. This result is in agreement with the increased levels initially observed for phoshocholine (a metabolite involved in the antioxidant protection of the cell membrane[47]) in the presence of AuChi NPs and confirmed previous findings[48]. Furthermore, phosphocholine is closely related to the metabolism of the cell membrane. As it has been previously described, both NPs exhibit opposite charges and this could lead to different interactions with the cell membrane. In fact, previous studies have reported that cationic NPs undergo a polycation-mediated endocytosis, thus implying a direct interaction with phospholipids and/or glycolipids in the membrane.[49] On the contrary, the interaction with negatively charged NPs would have to follow a more indirect approach.

Furthermore, the antioxidant system of the cell is closely related with the mitochondrial energy metabolism and, in particular with the TCA cycle, a process that was also altered in the presence of the NPs due to their antioxidant behaviour. For instance, alanine, aspartate and glutamine metabolism, related with the anabolism of the antioxidant gluthathione, was clearly affected by both NPs at similar time points. (Supplementary Figure 9) Alteration of this three metabolites in the presence of nanoparticles has already been reported in previous studies[24,45,46,50] and could be expected from the antioxidant properties of both AuChi and $AuCeO_2$ NPs. These metabolites can be introduced into TCA cycle by the aspartate-argininosuccinate shunt, indicating that this mechanism could be altered by AuNPs. Interestingly, the levels of

succinate and fumarate, two important TCA metabolites, experienced different effects in the presence of both NPs. Thus, while succinate and fumarate levels followed a similar pattern for control and $AuCeO_2$ treated cells, the tendency in AuChi treated cells was different, with decreased succinate levels and increased fumarate concentrations at 48h. These results showed that the effect of AuChi NPs (positively charged) on mitochondrial aerobic respiration was more pronounced than that induced by the negatively charged $AuCeO_2$ NPs, as it has already been observed in previous studies.[25,42] Taking into consideration that anaerobic glycolysis constitutes the main energy source for tumour cells, these results anticipate relevant properties for AuChi NPs, as they could generate a more oxidative environment against anaerobic proliferation. This finding would be also in agreement with the reduced levels of lactate, stemming from anaerobic respiration, observed in the presence of AuChi NPs, as opposed to the treatment with $AuCeO_2$ NPs that induced a slight increase in the levels of pyruvate, lactate and LDH.

Conclusions

$AuCeO_2$ and AuChi NPs have a significant impact, even at non-toxic levels, on cell metabolism, including the antioxidant mechanisms. Interestingly, although both NPs have a similar Au proportion and size, the presence of different stabilisers has a significant influence in their mode-of-action and the metabolic alterations induced by each of them. Thus, the results of this study suggest that AuChi NPs had a higher impact on aerobic respiration, while $AuCeO_2$ NPs seem to affect more the anaerobic energy pathways. The induction of specific metabolic alterations, even in the absence of cytotoxic effects, could have relevant implications in their biomedical applications (cancer, diabetes, cardiovascular diseases). From a methodological point of view, the study shows that metabolomic profiling of NPs by NMR could be a very useful approach to monitor the effects of these chemical entities in preclinical studies of nanomedicines, and could help to define their applications and toxicity with a focus on personalised treatments.

Conflicts of interest

There are no conflicts to declare.

Acknowledgements

This work was supported by the Carlos III Health Institute and the European Regional Development Fund (PI16/02064, CP13/00252) and the Spanish Ministerio de Economía y Competitividad (SAF2014-53977-R, SAF2017-89229-R and RD12/0036/0025). In addition, JRH is recipient of a contract from the Ministry of Health of the Carlos III Health Institute.

Bibliographic references & notes

1 J. Shi, P. W. Kantoff, R. Wooster and O. C. Farokhzad, *Nat. Rev. Cancer*, 2017, **17**, 20–37.

2 H. ju Yen, Y. an Young, T. neng Tsai, K. ming Cheng, X. an Chen, Y. chuan Chen, C. cheung Chen, J. jong Young and P. da Hong, *Carbohydr. Polym.*, 2018, **183**, 140–150.

3 S. Gioria, J. L. Vicente, P. Barboro, R. La Spina, G. Tomasi, P. Urbán, A. Kinsner-Ovaskainen, R. François and H. Chassaigne, *Nanotoxicology*, 2016, **10**, 736–748.

4 J. Beik, S. Khademi, N. Attaran, S. Sarkar, A. Shakeri-Zadeh, H. Ghaznavi and H. Ghadiri, *Curr. Med. Chem.*, 2017, **24**, 4399–4416.

5 N. M. S. Nagi, Y. A. M. Khair and A. M. E. Abdalla, *Jpn. J. Radiol.*, , DOI:10.1007/s11604-017-0671-6.

6 A. Gharatape and R. Salehi, *Eur. J. Med. Chem.*, 2017, **138**, 221–233.

7 E. Spyratou, M. Makropoulou, E. P. Efstathopoulos, A. G. Georgakilas and L. Sihver, *Cancers (Basel).*, 2017, **9**, 1–19.

8 M. H. ZHANG, J. Q. CHEN, H. M. GUO, R. T. LI, Y. Q. GAO, Y. TIAN, Z. J. ZHANG and Y. HUANG, *Chin. J. Nat. Med.*, 2017, **15**, 684–694.

9 J. Fang, H. Nakamura and H. Maeda, *Adv. Drug Deliv. Rev.*, 2011, **63**, 136–151.

10 K. Haume, S. Rosa, S. Grellet, M. A. Śmiałek, K. T. Butterworth, A. V. Solov'yov, K. M. Prise, J. Golding and N. J. Mason, *Cancer Nanotechnol.*, , DOI:10.1186/s12645-016-0021-x.

11 M. U. Farooq, V. Novosad, E. A. Rozhkova, H. Wali, A. Ali, A. A. Fateh, P. B. Neogi, A. Neogi and Z. Wang, *Sci. Rep.*, 2018, **8**, 1–12.

12 Y. Lin, Z. Wu, J. Wen, K. Ding, X. Yang, K. R. Poeppelmeier and L. D. Marks, *Nano Lett.*, 2015, **15**, 5375–5381.

13 C. Menchón, R. Martín, N. Apostolova, V. M. Victor, M. Álvaro, J. R. Herance and H. García, *Small*, 2012, **8**, 1895–1903.

14 P. Tiwari, K. Vig, V. Dennis and S. Singh, *Nanomaterials*, 2011, **1**, 31–63.

15 M. M. Fathy, F. S. Mohamed, N. S. Elbialy and W. M. Elshemey, *Phys. Medica*, 2018, **48**, 76–83.

16 X. Guo, Q. Zhuang, T. Ji, Y. Zhang, C. Li, Y. Wang, H. Li, H. Jia, Y. Liu and L. Du, *Carbohydr. Polym.*, 2018, **195**, 311–320.

17 Y. H. Lee, J. S. Kim, J. E. Kim, M. H. Lee, J. G. Jeon, I. S. Park and H. K. Yi, *Nanomedicine Nanotechnology, Biol. Med.*, 2017, **13**, 1821–1832.

18 I. C. Sun, J. H. Na, S. Y. Jeong, D. E. Kim, I. C. Kwon, K. Choi, C. H. Ahn and K. Kim, *Pharm. Res.*, 2014, **31**, 1418–1425.

19 P. M. Costa and B. Fadeel, *Toxicol. Appl. Pharmacol.*, 2016, **299**, 101–111.

20 M. Lv, W. Huang, Z. Chen, H. Jiang, J. Chen, Y. Tian, Z. Zhang and F. Xu, *Bioanalysis*, 2015, **7**, 1527–1544.

21 G. A. Nagana Gowda, G. A. Barding, J. Dai, H. Gu, D. H. Margineantu, D. M. Hockenbery and D. Raftery, *Front. Mol. Biosci.*, 2018, **5**, 1–13.

22 T. H. Shin, D. Y. Lee, H. S. Lee, H. J. Park, M. S. Jin, M. J. Paik, B. Manavalan, J. S. Mo and G. Lee, *BMB Rep.*, 2018, **51**, 14–20.

23 M. Palomino-Schätzlein, H. García, P. Gutiérrez-Carcedo, A. Pineda-Lucena and J. R. Herance, *PLoS One*, , DOI:10.1371/journal.pone.0182985.

24 J. Z. Lindeque, A. Matthyser, S. Mason, R. Louw and C. J. F. Taute, *Nanotoxicology*, 2018, **12**, 251–262.

25 Z. Liu, L. Wang, L. Zhang, X. Wu, G. Nie, C. Chen, H. Tang and Y. Wang, *Adv. Healthc. Mater.*, 2016, **5**, 2363–2375.

26 M. R. K. Ali, Y. Wu, T. Han, X. Zang, H. Xiao, Y. Tang, R. Wu, F. M. Fernández and M. A. El-Sayed, *J. Am. Chem. Soc.*, 2016, **138**, 15434–15442.

27 L. Zhang, L. Wang, Y. Hu, Z. Liu, Y. Tian, X. Wu, Y. Zhao, H. Tang, C. Chen and Y. Wang, *Biomaterials*, 2013, **34**, 7117–7126.

28 T. Esumi, K., Takei, N., Yoshimura, *Colloids Surf. B Biointerfaces*, 2003, **32**, 117–123.

29 S. Du, K. Kendall, P. Toloueinia, Y. Mehrabadi, G. Gupta and J. Newton, *J. Nanoparticle Res.*, , DOI:10.1007/s11051-012-0758-z.

30 E. L. Ulrich, H. Akutsu, J. F. Doreleijers, Y. Harano, Y. E. Ioannidis, J. Lin, M. Livny, S. Mading, D. Maziuk, Z. Miller, E. Nakatani, C. F. Schulte, D. E. Tolmie, R. Kent Wenger, H. Yao and J. L. Markley, *Nucleic Acids Res.*, 2008, **36**, 402–408.

31 D. S. Wishart, Y. D. Feunang, A. Marcu, A. C. Guo, K. Liang, R. Vázquez-Fresno, T. Sajed, D. Johnson, C. Li, N. Karu, Z. Sayeeda, E. Lo, N. Assempour, M. Berjanskii, S. Singhal, D. Arndt, Y. Liang, H. Badran, J. Grant, A. Serra-Cayuela, Y. Liu, R. Mandal, V. Neveu, A. Pon, C. Knox, M. Wilson, C. Manach and A. Scalbert, *Nucleic Acids Res.*, 2018, **46**, D608–D617.

32 T. Mosmann, *J. Immunol. Methods*, 1983, **65**, 55–63.

33 L. Yang, L. Shang and G. U. Nienhaus, *Nanoscale*, 2013, **5**, 1537–1543.

34 B. Zhitomirsky, H. Farber and Y. G. Assaraf, *J. Cell. Mol. Med.*, 2018, **22**, 2131–2141.

35 J. Chong, O. Soufan, C. Li, I. Caraus, S. Li, G. Bourque, D. S. Wishart and J. Xia, *Nucleic Acids Res.*, 2018, **46**, W486–W494.

36 A. A. Stepanenko and V. V. Dmitrenko, *Gene*, 2015, **574**, 193–203.

37 K. Suresh Babu, M. Anandkumar, T. Y. Tsai, T. H. Kao, B. Stephen Inbaraj and B. H. Chen, *Int. J. Nanomedicine*, 2014, **9**, 5515–5531.

38 M. Aldea, M. Potara, O. Soritau, I. S. Florian, A. Florea, T. Nagy-Simon, V. Pileczki, I. Brie, D. Maniu and G. Kacso, *J. B.U.ON.*, 2018, **23**, 800–813.

39 S. Y. Choi, S. H. Jang, J. Park, S. Jeong, J. H. Park, K. S. Ock, K. Lee, S. I. Yang, S. W. Joo, P. D. Ryu and S. Y. Lee, *J. Nanoparticle Res.*, , DOI:10.1007/s11051-012-1234-5.

40 T. G. de Carvalho, V. B. Garcia, A. A. de Araújo, L. H. da Silva Gasparotto, H. Silva, G. C. B. Guerra, E. de Castro Miguel, R. F. de Carvalho Leitão, D. V. da Silva Costa, L. J. Cruz, A. B. Chan and R. F. de Araújo Júnior, *Int. J. Pharm.*, 2018, **548**, 1–14.

41 J. Carrola, V. Bastos, J. M. P. Ferreira De Oliveira, H. Oliveira, C. Santos, A. M. Gil and I. F. Duarte, *Arch. Biochem. Biophys.*, 2016, **589**, 53–61.

42 E. Fröhlich, 2012, 5577–5591.

43 H. Gürer, H. Özgünes, E. Saygin and N. Ercal, *Arch. Environ. Contam. Toxicol.*, 2001, **41**, 397–402.

44 S. H. Lee, T. Y. Wang, J. H. Hong, T. J. Cheng and C. Y. Lin, *Nanotoxicology*, 2016, **10**, 924–934.

45 R. Saborano, T. Wongpinyochit, J. D. Totten, B. F. Johnston, F. P. Seib and I. F. Duarte, *Adv. Healthc. Mater.*, 2017, **6**, 1–13.

46 Y. Bo, C. Jin, Y. Liu, W. Yu and H. Kang, *Toxicol. Mech. Methods*, 2014, **24**, 461–469.

47 T. B. Shea, F. J. Ekinci, D. Ortiz, M. Dawn-Linsley, T. O. Wilson and R. J. Nicolosi, *Free Radic. Biol. Med.*, 2002, **33**, 276–82.

48 M. P. Schätzlein, J. Becker, D. Schulze-Sünninghausen, A. Pineda-Lucena, J. R. Herance and B. Luy, *Anal. Bioanal. Chem.*, 2018, **410**, 2793–2804.

49 A. C. Hunter, *Adv. Drug Deliv. Rev.*, 2006, **58**, 1523–1531.

50 C. Ratnasekhar, M. Sonane, A. Satish and M. K. R. Mudiam, *Nanotoxicology*, 2015, **9**, 994–1004.